OPEN ACCESS
International Journal of Neural Systems, Vol. 35, No. 6 (2025) 2550032 (21 pages)

DOI: 10.1142/S0129065725500327

World Scientific
www.worldscientific.com

Directed Weighted EEG Connectogram Insights of One-to-One Causality for Identifying Developmental Dyslexia

Ignacio Rodríguez-Rodríguez *,‡, José Ignacio Mateo-Trujillo *, Andrés Ortiz *,§, Nicolás J. Gallego-Molina *, Diego Castillo-Barnes * and Juan L. Luque †

*Departamento de Ingeniería de Comunicaciones
Universidad de Málaga, 29071 Málaga, Spain

†Department of Developmental and Educational Psychology
Universidad de Málaga, 29071 Málaga, Spain

‡ignacio.rodriguez@ic.uma.es

§aortiz@ic.uma.es

Received 31 October 2024
Accepted 25 March 2025
Published Online 9 May 2025

Developmental dyslexia (DD) affects approximately 5–12% of learners, posing persistent challenges in reading and writing. This study presents a novel electroencephalography (EEG)-based methodology for identifying DD using two auditory stimuli modulated at 4.8 Hz (prosodic) and 40 Hz (phonemic). EEG signals were processed to estimate one-to-one Granger causality, yielding directed and weighted connectivity matrices. A novel Mutually Informed Correlation Coefficient (MICC) feature selection method was employed to identify the most relevant causal links, which were visualized using connectograms. Under the 4.8 Hz stimulus, altered theta-band connectivity between frontal and occipital regions indicated compensatory frontal activation for prosodic processing and visual–auditory integration difficulties, while gamma-band anomalies between occipital and temporal regions suggested impaired visual–prosodic integration. Classification analysis under the 4.8 Hz stimulus yielded area under the ROC curve (AUC) values of 0.92 (theta) and 0.91 (gamma band). Under the 40 Hz stimulus, theta abnormalities reflected dysfunctions in integrating auditory phoneme signals with executive and motor regions, and gamma alterations indicated difficulties coordinating visual and auditory inputs for phonological decoding, with AUC values of 0.84 (theta) and 0.89 (gamma). These results support both the Temporal Sampling Framework and the Phonological Core Deficit Hypothesis. Future research should extend the range of stimuli frequencies and include more diverse cohorts to further validate these potential biomarkers.

Keywords: Causality networks; functional connectivity; connectogram visualization; developmental dyslexia.

§Corresponding author.

1. Introduction

Developmental dyslexia (DD) is a shared learning problem in about 5–12% of pupils imposing significant challenges in reading and writing despite normal intelligence levels.[1] Characterized by challenges like letter migration and frequent spelling errors, DD can occur with no apparent connection to the level of intelligence and educational capabilities. Traditionally, diagnostics is highly dependent on behavioral tests of reading and writing skills. However, these assessments are sensitive to exogenous factors such as individual attitudes, dedication, and contextual variables, including mother tongue and learning levels. This leads to unreliable diagnosis.[2] In response, there is an urgent need for objective diagnostic standards that are independent of such external influences.

A promising path is the development of systems not influenced by the student's behavior and context. For example, using auditory stimuli simulating speech, such as white noise modulated at frequencies corresponding to the language envelope, helps to identify differences in brain areas active during auditory processing between dyslexic and nondyslexic individuals. This approach can provide valuable insights into the neurophysiological underpinnings of DD, especially in how the brain processes speech prosody and phonemic elements.

Dyslexia is linked to a range of behavioral symptoms, including increased anxiety, depressive tendencies, low self-esteem, rule-breaking, aggressiveness, attentional deficits, and hyperactivity, with personality traits showing higher neuroticism and lower extroversion.[3] While integrating detailed behavioral data with biological data could offer a fuller understanding of these manifestations, it implies subjective behavioral assessments.[3] There are different neuroimaging methods for collecting functional brain data, including functional magnetic resonance imaging (fMRI), magnetoencephalography (MEG), and functional near-infrared spectroscopy (fNIRS).[4] However, electroencephalography (EEG) remains the most widely used and cost-effective method for assessing cortical brain activity with high temporal resolution.[5] EEG measures electrical activity over different frequency bands. It is striking that stimulation in one band can influence the activity in others through the complex oscillating dynamics of the brain. Examining the patterns that emerge separately in these bands can provide valuable insights into the neural mechanisms associated with DD.[6]

EEG is based on studies investigating functional network connectivity and brain structure in dyslexia. Functional connectivity pertains to the level of synchronization between activities in different brain areas during task engagement and reflects the coordinated activity among distinct regions. Earlier research has used several EEG-based techniques to assess functional connectivity, focusing on identifying patterns typical of brain disorders, including Parkinson's disease[7] and other neuro disorders.[8] Connectivity analysis allows deeper insights by examining parameters that connect signals from different brain regions, such as correlation, causality, and covariance.[9] This approach is consistent with the idea that the brain works as a hyper-connected network,[10] where regions influence each other through direct interactions and phase or phase amplitude modulations between frequency bands.[11]

Based on this framework, we propose extracting each EEG band's frequency components from the signals obtained under the stimuli (a phonetic stimulus at 40 Hz alongside the prosodic 4.8 Hz stimulus). These components can then be used to create a pattern of linkage based on causality between Granger channels.[12] Granger's causality (GC) link is a statistical method to determine whether a time series can predict another, thus providing insight into the directional influence between brain regions. The objective of this study is to assess EEG-based one-to-one GC models as objective diagnostic markers for DD, with the hypothesis that distinct connectivity patterns differentiate dyslexic from nondyslexic individuals, providing deeper insight into the neural mechanisms underlying their phonological and prosodic processing difficulties.[13] Furthermore, enhanced visualization using connectograms enables detailed representation of both the direction and strength of neural connections, clearly highlighting differences between dyslexic subjects and controls. Moreover, the integration of methods of selection of characteristics, such as the Mutually Informed Correlation Coefficient (MICC) with machine learning classifiers, can effectively distinguish between control subjects and study subjects in scientific experimentation.[14] Robustness of

the classification analysis was also improved by performing extensive permutation tests and reporting detailed performance metrics. This expanded approach situates our findings within the broader literature on DD, complementing both the Temporal Sampling Framework (TSF) and the Phonological Core Deficit Hypothesis (PCDH).

Previous research revealed the significant role of neural oscillations in phonological processing and speech perception, suggesting that the deficiencies of these oscillations contribute to the phonological difficulties observed in dyslexic individuals. The TSF shows that phonological deficits in DD result from atypical neural oscillations that disrupt auditory information processing in different frequency bands.[15] These findings can also be interpreted through the lens of the more traditional PCDH,[16] which posits that DD emerges from unstable or imprecise mental representations of speech sounds, thus complicating the mapping between letters (graphemes) and sounds (phonemes). In particular, altered connectivity in fast/slow bands under different auditory envelopes can be understood as a neural manifestation of deficient phonological processing.[17]

The connectivity analysis extends beyond interrelations between brain areas; regions can influence each other through phase–phase or phase–amplitude modulations between frequency bands.[11]

Despite advances in some areas of biomedicine, using advanced visualization techniques such as connectomes remains relatively rare for investigating dyslexia. Interestingly, these tools have shown great promise when applied to other neurological disorders.[18] Connectomes provide a visual representation of brain connectivity patterns, thus facilitating the interpretation of complex neural networks.[19] In this context, our study uniquely contributes by leveraging advanced EEG-based connectivity analysis and connectogram visualization to address the diagnostic challenges of DD.

After this introductory section, the paper continues with a Sec. 2 where relevant literature is presented, followed by Sec. 3 where the origin of the data and the methodology are duly explained. Section 4 presents the results and their discussion, detailing them according to stimulus, and discusses the different brain activity between controls and study subjects by affected bands and brain regions. The paper finishes with interesting conclusions and possible future work in Sec. 5.

2. Related Works

Research into the neurophysiological support of DD has shown how disorders in neural oscillations contribute to phonological problems, with central importance placed on the disruption in processing speech prosody and syllabic–phonemic elements. Specifically, atypical oscillatory activity occurs in brain regions responsible for the temporal aspects of speech, affecting both the low-frequency prosodic properties and the higher-frequency phonemic signals, which are linked to the language challenges dyslexic learners face. Studies[20] suggest that reduced coding of low-frequency speech covers, which contain crucial prosodic information, broadly supports problems in tasks requiring prosodic awareness, such as identifying syllable stress.[21] At the same time, research shows that dyslexic individuals exhibit disturbances in the phonemic processing associated with oscillating deficits in higher frequencies, such as the gamma band, which facilitates rapid neural synchronization essential to phoneme recognition.[22] These findings suggest that delta and theta[23] bands are crucial for synchronizing neural activity during speech processing at lower frequencies, while gamma oscillations support phonemic processing at higher speeds.[17]

Further research into the biological mechanisms of DD suggests that it is characterized by atypical neural entrainment of the slow prosodic (0.5–1 Hz), syllabic (4–8 Hz), and phonemic (12–40 Hz) rhythms in speech.[24] This atypical oscillating sampling disrupts the ability of individuals with DD to capture linguistic units, leading to reduced phonological representations. However, it is essential to note that these distortions are not uniform across all frequency bands. Recent studies show that different connectivity patterns across different frequency bands (delta, theta, alpha, beta, and gamma) arise in persons with DD.[4]

EEG has played an influential role in studying these oscillating abnormalities in DD, which gives insight into how individuals process auditory and speech stimuli with dyslexia. Power *et al.*[20] used noise-encoded speech in EEG studies to degrade

speech signal's temporal fine structure while maintaining the low-frequency envelope, meaning participants had to rely mainly on this information for word recognition. Their findings showed that individuals with DD have a reduced ability to reconstruct signal speech envelopes, indicating damage in time sampling of prosody. This supports the TSF, which states that phonological deficits in DD arise from atypical neural oscillations, disrupting the time processing of auditory information across different frequency bands.

Building on these findings, EEG research has increasingly focused on the specific role of different frequency bands in processing prosodic and phonemic elements in speech. Disruptions in theta-band synchronization have been consistently observed in dyslexic individuals during prosodic language tasks, especially in response to stimuli evoking prosody at a frequency of 4.8 Hz closely linked to rhythmic and prosodic processing.[25] These disturbances suggest that a core deficiency in DD lies in the brain's ability to integrate temporary information about longer windows, crucial to the perception and production of rhythm and speech intonation.[26]

In addition to the theta band, the gamma-band oscillations facilitate rapid synchronization between distributed brain regions,[27] enabling sensory and cognitive information needed to decode phonemic and prosodic speech elements.[28] Research has shown that individuals with DD show significant changes in gamma-band connectivity during tasks requiring the perception of phonemes or prosody, particularly when exposed to a 40 Hz stimulus, which is closely linked to phoneme perception.[29] These disturbances in gamma cohesion indicate a broader dysfunction in the neural mechanisms underlying speech processing in dyslexia. The theta–gamma clutch mechanism has attracted much attention in recent research as it investigates how interactions between slower theta oscillations and faster gamma oscillations contribute to phonological deficits. Theta oscillations are assumed to modulate the timing of gamma oscillations, which are crucial for phonemic processing and multisensory integration.[22] In dyslexic subjects, damage in this entrainment between theta and gamma interaction can explain how lower frequency disturbances cascade to higher-frequency deviations and affect prosodic processing over multiple levels.[20]

Connectivity analysis has helped to determine the relationship between brain regions in different frequency bands.[30] Methods used to measure connection interference in dyslexia include coherence, phase-locking value (PLV), or GC.[31] Žarić *et al.*[13] investigated connectivity models between visual and language processing networks for dyslexic individuals using visual names and fake font processing tasks. When calculating the power spectral density (PSD) across individual EEG bands, they found significant interference in the connection of brain regions involved in language processing during reading tasks.[32] One of the most effective methods for brain connectivity analysis in EEG studies is phase synchronization analysis. This approach involves measuring the level of alignment of the two-signal phase, which provides insight into the coherence of the brain regions. Mormann *et al.*[33] revealed that fluctuations in phase synchronization are often prior to epileptic seizures, suggesting that phase synchronization analysis may also help detect early signs of dysregulation in other circumstances, including DD. Granger's causing relationships have been widely used to explore cerebral relationships. Unlike conventional correlation measures, Granger rates whether a series can be predicted by another one that provides a nourished understanding of the directional connection in the brain. This technique was successfully used in neural science research to evaluate the joint of the brain in many conditions, including emotion recognition[34] or vagus nervous stimulation.[35] In dyslexia, Granger's causing relations have been shown to communicate with various brain areas in the language.

Previous research has explored the use of nonlinear GC to capture neural dynamics in more sophisticated ways.[36] However, these nonlinear approaches often require substantial computational resources, along with tailored configurations for each specific application, and they typically rely on iterative trial-and-error during development.

The selection methods have played a vital role in this high-dimensional EEG scenario. MICC has been developed to identify the most innovative functions while minimizing redundancy.[37] MICC combines Mutual Information (MI) with Pearson's Correlation Coefficient (PCC). MI measures the dependency between each EEG feature and the class label

(dyslexic or nondyslexic), helping to identify the most informative features that contribute to distinguishing between the two groups. On the other hand, PCC assesses the linear correlation between pairs of EEG features, enabling the detection and removal of highly correlated (redundant) features that do not provide additional discriminatory power.[14]

Graph theory has also been used to analyze connectivity patterns during language tasks. González *et al.*[38] used the graph theory to compare EEG connectivity to audiovisual players and at rest. They observed significant differences in connectivity patterns between dyslexia and typical learners, suggesting that dyslexia is associated with altered network dynamics during language processing tasks. Also, Bosch-Bayard *et al.*[39] demonstrated that effective connectivity has been changed for persons with DD, which indicates a disruption of information flows between brain regions responsible for timing and phonetic processing. Connectograms have become an invaluable tool for visualizing brain connectivity models. These circular diagrams represent brain nets, with nodes representing brain regions and edges representing their compounds. Recent studies have used connectograms to highlight differences in connectivity between different brain disorders,[18] as many studies have revealed organizational and topological characteristics in several brain disorders, such as Alzheimer's disease,[40] minor cognitive impairments,[41] Parkinson's disease,[42] epilepsy,[43] autism,[44] borderline intellectual activities[45] or depression.[46] However, the use of connectograms in dyslexia remains very limited.

Progress in the analysis of EEG connectivity, including GC, phase synchronization, and connectograms, has significantly improved our understanding of the neural mechanisms that underpin the development of dyslexia. Integrating machine learning techniques with EEG connectivity analysis is a great promise to identify the main neural signatures of DD, offering possible ways to improve diagnostic and intervention strategies.

3. Experimental Setup and Methodology

3.1. *Data collection*

The EEG dataset comes from the Leeduca study group at the University of Malaga (Málaga, Spain)[47] and comprises 97 children between 88 and 100 months ($t(1) = -1.4,\ p > 0.05$). This cohort consisted of 67 skilled and 30 dyslexic readers, all right-handed and native speakers with normal or corrected vision and no auditory disorders. The children diagnosed with dyslexia in the study received their formal diagnosis at school. Conversely, the competent readers showed no signs of reading or writing challenges and had no DD diagnosis.

DD frequently co-occurs with other neurodevelopmental disorders, particularly ADHD, with high comorbidity rates. This suggests that these conditions may not be entirely separate disorders but rather symptoms of broader developmental delay syndromes.[48] To minimize the risk of comorbidities in our sample, we drew upon a large cohort of 2000 students and performed individualized assessments of foundational cognitive processes for reading acquisition (IQ, working memory, phonological awareness, vocabulary, oral comprehension, rapid naming, morphosyntax, etc.). All variables underwent standardization to remove scale-related biases. Subsequently, hierarchical cluster analysis followed by confirmatory k-means clustering was employed to identify four distinct cognitive-linguistic profiles: (a) dyslexia risk, (b) specific language impairment risk, (c) comorbid risk, and (d) controls. Critically, we only retained EEG data from participants situated beyond ± 1.5 standard deviations in the relevant cognitive measures that aligned with "pure" dyslexia risk versus controls, thus excluding individuals who showed overlapping traits with other neurodevelopmental disorders.

Before taking part, the guardians of the children were informed about the objectives of the study, provided formal consent, and accompanied their departments over the course of the experiment.

Volunteers were exposed to auditory stimuli during sessions. These stimuli were white noise with separate modulations at 4.8 Hz and 40 Hz, each of 2.5 min. The selection of these specific frequencies aimed to distinguish synchronization patterns caused by the fundamental auditory processing. Linguistic psychologists' expertise further informed the choice of the predominant frequency components of prosodic and phonemic qualities in human speech.

The selection of 4.8 Hz and 40 Hz modulation rates for investigating auditory processing in DD

stems from the fact that these frequencies closely correspond to two key temporal windows in speech perception. Slower modulations around 4–5 Hz capture the prosodic or syllabic rhythm, while faster modulations around 30–40 Hz align with the rapid acoustic cues essential for phonemic distinctions.[49] Empirical findings support this dichotomy: for example, Lehongre and colleagues[50] demonstrated that individuals with dyslexia exhibit an abnormal reduction in left-hemisphere entrainment at $\sim$ 30 Hz, indicating a deficit in phonemic-rate processing. Conversely, other research has reported that dyslexic individuals often display atypical sensitivity to slower ($\sim$ 4 Hz) modulations, affecting syllable timing and prosody. Hämäläinen *et al.*[51] observed reduced-phase-locking to $\sim$ 4 Hz amplitude-modulated sounds in adults with dyslexia, aligning with a deficit in syllabic parsing. Taken together, these studies suggest that 4–5 Hz and $\sim$ 30–40 Hz stimuli each isolate a distinct level of linguistic processing — syllabic/prosodic versus phonemic — both of which may be impaired in dyslexia.

EEG signals from the participants were collected using a BrainVision actiCHamp Plus, equipped with 32 active electrodes (actiCAP, Brain Products GmbH, Germany), and were sampled at a speed of 500 Hz.

3.2. *Preprocessing*

Preprocessing EEG signals required removing artifacts related to eye blinks and variations due to movement or impedance. Eye-blinking artifacts were treated using Independent Component Analysis (ICA),[52] guided by eye movement observations in the electrooculography (EOG) channel. Segments EEG, which showed movement or impedance variations, were then discarded. After these corrections, EEG channels were normalized to the Cz electrode.

EEG channels then had band-pass filtering to record data on the five EEG frequency bands. We employed finite impulse response (FIR) filters due to their ability to maintain a consistent phase delay, which can then be adjusted. In detail, signals were processed employing a two-way zero-phase band-pass FIR least-squares filter, both forward and backward. This approach provided a comprehensive zero-lag phase in filtering, addressing the problems related to potential phase delay.[53] In addition to using an 80 Hz low-pass filter, a 50 notch Hz filter was integrated during preprocessing to prevent this specific frequency component.

3.3. *Hilbert transform*

In our methodology, we employed the Hilbert transform, a valuable tool for time–frequency analysis, to process the EEG channels. The primary aim was to extract the instantaneous phase component from the EEG signals. Mathematically, given a signal $x(t)$, its Hilbert transform $\hat{x}(t)$ is defined as

$$\hat{x}(t) = \frac{1}{\pi} \int_{-\infty}^{+\infty} \frac{x(\tau)}{t-\tau} d\tau. \quad (1)$$

By combining $x(t)$ and $\hat{x}(t)$, the analytic signal $z(t)$ is formulated as

$$z(t) = x(t) + i\hat{x}(t). \quad (2)$$

From this, the instantaneous phase $\phi(t)$ is derived using the arctangent function

$$\phi(t) = \arctan \frac{\hat{x}(t)}{x(t)}. \quad (3)$$

The subsequent analysis is based on the phase component, $\phi(t)$, and provides a more complicated glimpse of oscillating brain functions. With a phase-centric perspective, this method brings forward an understanding that cannot reach conventional techniques. It paves the way for recognizing subtle patterns and synchronizations crucial to EEG behavior.

3.4. *Granger causality*

GC is a pivotal statistical hypothesis test to determine whether one time series can predict another.[54] Instead of being causality in a philosophical sense, it operates on the premise that if a variable X Granger-causes a variable Y, then past values of X contain information that helps predict Y.

Considering EEG signals after their transformation via the Hilbert method, let us address the application of GC to these phase components. The prime approach is to employ Vector Autoregressive (VAR) models. A VAR model of order p (VAR(p)) for n time series X_t (number of channels) is represented as

$$X_t = A_1 X_{t-1} + A_2 X_{t-2} + \cdots + A_p X_{t-p} + \in_t, \quad (4)$$

where X_t is an $n \times 1$ vector of observations at time t, A_i denotes $n \times n$ coefficient matrices, and $\in_t$ is an $n \times 1$ white noise error vector.

For the selection of the optimal choice of the VAR model order p, the Akaike Information Criterion (AIC)[55] is expressed as

$$\mathrm{AIC}(p) = \ln |\Sigma_p| + \frac{2kp}{T}, \tag{5}$$

where Σ_p is the residual covariance matrix of the VAR(p) model, k is the number of variables, and T is the number of observations. The optimal order p^* is that which minimizes the AIC

$$p^* = \mathrm{argmin}\ \mathrm{AIC}(p). \tag{6}$$

With p^* established, it is possible to proceed with the GC computations, discerning whether the past of one EEG channel's phase component can predict another's

$$Y_t = \sum_{i=1}^{p} B_i Y_{t-i} + \in_t, \tag{7}$$

$$Y_t = \sum_{i=1}^{p} A_i X_{t-i} + \sum_{i=1}^{p} B_i Y_{t-i} + \in_t' . \tag{8}$$

The F-test[56] contrasts with these models to determine whether including previous X values significantly improves Y's prediction. We conducted GC analyses for each participant to get into the interaction between channels, offering an $n \times n$ matrix filled with p-values, where n represents the total amount of electrodes.

We are discerning oscillatory coordination patterns in neural systems by analyzing GC in the phase components of EEG channels. This provides a nuanced understanding of how dissimilar brain regions intercommunicate, and when they are extended to clinical contexts such as DD, they can provide prospects for transformation into diagnosis and therapeutic interventions.[57,58]

3.5. *MICC for feature selection*

MICC is a new filter-based Feature Selection (FS) method designed to efficiently select essential features of high-dimensional function vectors,[37] which ensures the explainability of our proposal. This method takes into account both the feature–feature correlation and the feature–class correlation in order to extract the different properties that are relevant to the problem. In this way, rather than studying individual profiles of specific subjects, it is possible to identify the most discriminating causal connections in the EEG data, i.e. those that transcend the common characteristics of people with dyslexia.

MICC is based on MI, a quantity of information that can be provided by one of the variables. In FS, the MI measures the dependency between a feature and a class label. The higher the MI value, the more informative the feature in the class tag. It is defined as

$$\mathrm{MI}(A;B) = \sum_x \sum_y p(a,b) \log_{10}\left(\frac{p(a,b)}{p(a)p(b)}\right), \tag{9}$$

where A and B are two random variables, $p(a,b)$ is the joint probability distribution of A and B, and $p(a)$ and $p(b)$ are the marginal probability distributions of A and B, respectively.

The MI ranges from 0 to ∞, where a value of 0 indicates no dependence between the variables, and higher values indicate stronger dependence. The MICC method uses MI to measure the degree of dependence between a feature and the class label C, so in Eq. (9), let A be a feature called X and B be the class label called C.

MICC also utilizes PCC to measure feature–feature correlation. PCC is a linear connection measure between two variables. The PCC measures the degree of correlation between two features concerning the FS. The higher the PCC value, the more correlated the two features. This is defined as

$$\mathrm{PCC}(x,y) = \left(\frac{1}{n-1}\right) \sum_{i=1}^{n} \frac{(x_i - \bar{x})(y_i - \bar{y})}{s_x s_y}, \tag{10}$$

where n is the number of samples, x_i and y_i are the values of the two variables for the ith sample, $\bar{x}$ and $\bar{y}$ are the means of the two variables, and s_x and s_y are the standard deviations of the two variables.

The PCC ranges from -1 to 1, where a value of -1 indicates a perfect negative correlation, 0 indicates no correlation, and 1 indicates a perfect positive correlation.

MICC combines hence MI and PCC values to bring a score to each feature. The score reflects the extent of the interrelation between the feature and the class label and the extent of the connection between the feature and other features in the vector.

Then, the features are ranked according to the scores, and the upper-ranking features are selected for further analysis. The MICC score for feature i is defined as

$$\text{score}(i) = \alpha \times \text{MI}(i) - (1-\alpha) \times \sum_{j=1}^{\dim} \text{PCC}(i,j), \tag{11}$$

where $\text{MI}(i)$ is the MI between feature i and the class label C, and α is a parameter that controls the trade-off between MI and PCC.

The MICC method first computes the MI between each feature and the class label. Then, it computes the PCC between each pair of features. Finally, the MICC method computes the score for each feature and ranks the features based on their scores. The top-ranked features are selected for further analysis.

Unlike traditional methods that consider either MI or redundancy in isolation, MICC integrates both metrics into a single score, providing a more intuitive and balanced evaluation of each feature's utility. Another advantage of MICC is that it is a classifier-independent method, meaning it can be used with different classifiers without affecting performance. Also, MICC is computationally efficient and can handle high-dimensional feature vectors, a common problem in many real-world applications. Furthermore, MICC is a flexible method that can be extended to other standard correlation coefficients like Spearman and Kendall. It can also be applied to various pattern classification problems, including handwritten document image classification, text classification, and image recognition. MICC reduces the computational complexity and the number of features required.

3.6. *Machine learning classifier*

Ensemble methods are approaches that are sufficiently robust to improve predictions and have also been found to be stable.[59] In essence, ensemble methods integrate several models, each with its predictive capability. Thus, the prediction is not based on a particular model but merges the individual predictions, usually with a weighted majority vote that forms the final prediction. The performance of the algorithm simply identifies the most discriminating stimulus-band scenario, where there are more differences between groups. That is, where very different language processing will be observed in the study group.

Originally, each training sample is shown with equal weight, symbolically represented as $w_i = 1/N$. Initial training of the weaker learner is based on raw, unchanged data. However, as the boosting process iterates, these weights transform. Specifically, trained cases that minimize prediction accuracy experience an increase in their weights. Conversely, examples predicted with precision are assigned a reduced weight. This iterative change of sample weights ensures that challenging examples, which were initially challenging to predict, gradually have a more significant impact. Thus, the successful weak learners are systematically sent to emphasize previously overlooked samples. The culmination of these steps ensures that ensemble methods exploit both the diversity and the power of multiple learners, creating an increased focus on complex data patterns that can be missed by some models, resulting in superior predictive results.

Ensemble techniques have cut a niche in machine learning, consistently perform standalone models, especially in scenarios that require enhanced accuracy for binary predictions on limited datasets.

One of the prominent ensemble techniques employed in our study is the Gradient Boosting (GB) classifier.[60] This method constructs an additive model in an iterative manner by optimizing the logistic loss function for binary classification. Specifically, for a training dataset $\{(x_i, y_i)\}_{i=1}^{N}$, with $y_i \in \{0,1\}$, the logistic loss is defined as

$$L(y, f(x)) = \sum_{i=1}^{N} \left[y_i \log_{10}\left(\frac{1}{1+e^{-f(x_i)}}\right) + (1-y_i)\log_{10}\left(\frac{1}{1+e^{-f(x_i)}}\right)\right]. \tag{12}$$

At each boosting iteration m, the model $f_m(x)$ is updated by fitting a regression tree $h_m(x)$ to the negative gradient (pseudo-residuals) of the loss function

$$r_{im} = -\left[\frac{\partial L(y_i, f(x_i))}{\partial f(x_i)}\right]_{f(x)=f_{m-1}(x)}. \tag{13}$$

These pseudo-residuals indicate the direction of steepest descent in the loss function. The regression tree $h_m(x)$ approximates these residuals, and the

model is updated as follows:

$$f_m(x) = f_{m-1}(x) + \eta h_m(x), \tag{14}$$

where η is the learning rate that scales the contribution of each tree. This iterative process is repeated for a predetermined number of rounds M, resulting in the final model

$$f(x) = f_0(x) + \eta \sum_{m=1}^{M} h_m(x). \tag{15}$$

For binary classification, this approach is particularly effective as it iteratively refines the decision boundary between the dyslexic and control groups. Each shallow regression tree contributes modest corrections to the model, cumulatively enhancing predictive performance while mitigating overfitting.

We used Python's scikit-learn library (version 1.6.1) to implement a GB classifier, optimizing its hyperparameters (Table 1) through a grid search. In order to ensure strong generalizability and to mitigate overfitting, the dataset was partitioned into 20 subsets (20-fold cross-validation). Stratification is necessary to minimize the impact of database imbalance. During each iteration, the model was trained on 19 folds and validated on the remaining fold. This process was repeated until every fold had served once as the validation set, thereby providing a comprehensive measure of the classifier's performance. Accuracy was calculated as the ratio of correct predictions ($y_{\text{pred}} = y_{\text{true}}$) over the total number of samples in each validation fold. For the area under the receiver operating characteristic (ROC) curve (AUC), we applied scikit-learn's built-in roc_auc_ score function, which integrates the true-positive rate versus false-positive rate across all decision thresholds.

Table 1. Classifier parameter grid.

Algorithm	Parameter	Interval
GB	ntrees	[50, 100, 200, 500]
	max_depth	[3, 5, 7, 10]
	min_rows	[1, 5, 10, 20]
	learn_rate	[0.001, 0.01, 0.05, 0.1]
	sample_rate	[0.6, 0.8, 0.9, 1.0]
	col_sample_rate	[0.6, 0.8, 1.0]

3.7. *Connectograms for visual representation*

Within the realm of neuroscience, connectograms serve as an invaluable tool to represent complex brain connectivity patterns. Originating from fMRI studies, these graphical representations have found their application extended to EEG data as well.[19] The myriad of interconnected nodes and pathways in an EEG connectogram holds a mirror to the intricate neural connections and the underlying brain activity.

Incorporating the notion of directed and weighted graphs into EEG connectograms offers a more nuanced insight into these interactions. In this context, a directed graph accounts for causality, mainly when inferred from GC measures, which may not be symmetric. In simple terms, while electrode A might influence electrode B to a certain degree, the reverse influence of B on A could be of a different magnitude or perhaps even nonexistent.[54] This directional nature of influence is crucial when studying interactions between EEG channels, as it can reveal which areas of the brain might be driving activity in others.

The weighting in these graphs takes the form of GC values, signifying the strength or likelihood of a causal relationship between two nodes. A higher weight (or a lower value in GC, indicating stronger causality) on an edge connecting two nodes implies a more substantial causal influence between the respective EEG channels. Conversely, a lower weight suggests a weaker or more uncertain causal link.[12]

Utilizing a weighted and directed graph to represent EEG connectograms ensures that the derived representation is not just an oversimplification of the complex interactions but a more true-to-reality depiction. Connectograms can also be used to visually represent any other brain variables that enclose direction between electrodes and magnitude. In this sense, the most discriminating connections between control and dyslexic groups can also be represented, indicating the scores achieved in the FS ranking. The conversion of the well-known topoplot representation into a connectogram is shown in Fig. 1. Following a criterion of proximity and belonging to a particular region, the electrodes are connected and opened to form a circle.

3.8. *Methodological outline*

Therefore, the Hilbert transform of each electrode is performed on the EEG signals. For each subject,

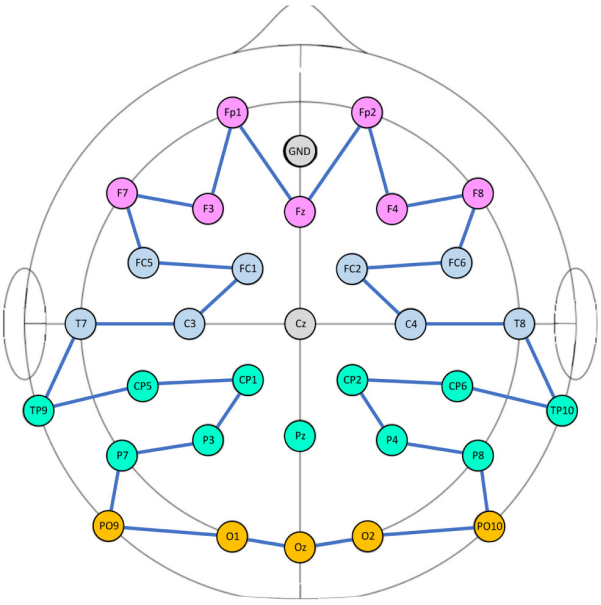

Fig. 1. Diagram of electrode connections for transformation into a connectogram.

causality matrices are calculated, resulting in a high-dimensional space that is reduced and ranked according to the MICC method. The most relevant variables are used to classify the subjects according to a machine learning classifier, thus assessing how discriminant is the selected subset of the feature space. Both the causality matrices and the selection of the most discriminating features can be represented and visualized in connectograms. Algorithm 1 summarizes this schema.

Algorithm 1. Methodological outline

For each participant:
  Present auditory stimuli:
    Stimulus1 ← White noise modulated at 4.8 Hz
    Stimulus2 ← White noise modulated at 40 Hz
  Record EEG signals during stimuli presentation
  Preprocess EEG signals:
  For each frequency band in [δ,θ,α,β,γ]:
    Filter EEG_fb signals
    Compute HT and Extract instantaneous phase:
      AnalyticSignal ← HilbertTransform (EEG_fb)
      Phase_fb ← arctangent (Im(z)/Re(z))
  End For
  Compute Granger Causality:
    Determine optimal VAR model order p* using AIC
    For each pair of EEG_fb channels (i, j):
      Fit VAR(p*) models to Phase_fb
      p_value ← GrangerCausalityTest (Phase_i, Phase_j)
      CausalityMatrix[i][j] ← p_value
    End For
  Flatten CausalityMatrix into FeatureVector
  Label ← Participant's class (dyslexic or skilled reader)
End For
Aggregate all FeatureVectors and Labels into Dataset

For stimuli in [4.8 Hz, 40 Hz]:
  For each frequency band in [δ,θ,α,β,γ]:
    Compute Mutual Information (MI):
    For each feature i: MI[i] ← MI(feature i, class labels)
    Compute Pearson Correlation Coefficient (PCC):
    For pair of features (i, j): PCC[i][j] ← PCC(f_i, f_j)
    Compute MICC Scores:
    For each feature i:
      Score[i] ← $\alpha \times$ MI[i] $-$ $(1-\alpha) \times \Sigma$_j PCC[i][j]
    Rank features based on Score[i]
    Select top N features for classification
    Train Gradient Boosting Classifier:
    Input: Selected top N features, Labels
    Optimize hyperparameters
    Evaluate classifier performance (Accuracy, AUC)
    Visualize Networks:
    For each group Create connectogram.
    Nodes ← EEG electrodes Edges ← connections
  End For
End For

4. Results and Discussion

Once we have obtained causal relationships between electrodes for each subject, we face the challenge of optimally visualizing this interaction. Given that these interactions are oriented and weighted, these matrices are asymmetrical with regard to the diagonal.

One method of simplifying these complex matrices is to reduce the dimensionality through Principal Component Analysis (PCA). By keeping enough principal components to achieve a significant level of explained variance, we may try to display the data in traditional topoplots. Other techniques like t-distributed Stochastic Neighbor Embedding (t-SNE) can be particularly adept at revealing local clusters in data such as images or large textual embedding. However, such simplification often leads to a loss of relevant information. Electrodes generate both giving and receiving causality, in the form of positive and negative effects, so that these effects compensate each other in this simplification. Consequently, the principal components of the same magnitude, but opposite direction can be compensated and overshadowing relevant causality data. An example of this representation can be seen in Fig. 2. where the

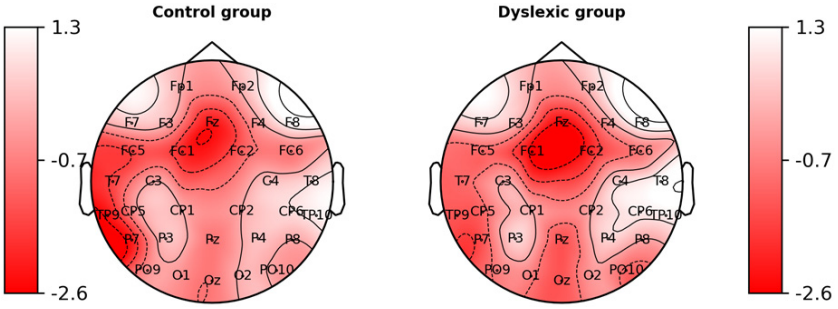

Fig. 2. Average activity reduced by PCA in theta band for 40 Hz stimulus.

activity in the theta band, reduced by PCA, is plotted for a 4.8 Hz stimulus (average, control, and study group).

To overcome this constraint, more complex representations such as connectograms are used, they allow simultaneous visualization of both incoming and outgoing causalities between electrodes using arrows to indicate the direction of impact. The strength of these causal compounds is represented by the thickness of the arrows, which gives a quantitative measure of the extent of the interaction. This approach preserves the intricate details of the causal network, but it may overlook the more streamlined and informative visualization that simpler methods could offer.

Although the choice of only two discrete modulation rates (4.8 Hz and 40 Hz) facilitates a focused investigation into syllabic/prosodic versus phonemic-level processing, it inevitably leaves out other potentially relevant temporal cues. Real speech encompasses a hierarchy of rhythms, from slower intonation (1–2 Hz) to intermediate onset-to-onset intervals (8–20 Hz). Studies that have expanded the frequency range, such as Lizarazu *et al.*,[49] reveal dyslexic abnormalities at multiple rates, indicating that temporal impairments may be broad rather than confined to a single band. Nonetheless, 4.8 Hz and 40 Hz serve as a theoretically grounded starting point, allowing a direct examination of directed connectivity at two critical scales. Future research would benefit from incorporating additional or continuously varying stimuli to further elucidate the full spectrum of dyslexic temporal processing.

The strength of the causal relationships is shown in Fig. 3, also representing the average causal activity for the control group and the group of people with dyslexia in theta band for 4.8 Hz stimulus. Note how the hemispheric lateralisation[61,62] is more clearly observed for controls, and the higher activity in the dyslexic group.[63]

4.1. *Stimulus at 4.8 Hz (Prosody)*

Once all the methodological steps outlined in Sec. 3.8 have been completed, we obtain performance metrics, obtained in different subsets of features (the n most relevant), and it is observed that the best classifications (that is, where the highest discrimination is observed) are in the theta and gamma bands, as it is marked in Table 2.

The analysis of brain response to a 4.8 Hz stimulus, adapted for language prosody, shows significant differences in functional connectivity between electrodes in individuals with dyslexia compared to controls, especially in prosodic language processing.[64] The theta band is critical for the coordination of attention, working memory, and temporal synchronization of neural activity, which are essential for correctly interpreting rhythm and speech intonation. The dysfunction in theta synchronization observed in people with dyslexia may indicate a change in the brain's ability to temporarily integrate information, affecting the perception of rhythm and tone, which are the key to prosodic understanding.[25,65] Table 3 shows the hyperparameters set.

Hereon, we will focus on these two bands in the presentation of results and discussion. Table 2 shows the results, and we can observe the evolution of the ROC curves in Fig. 4.

In individuals with dyslexia, the connections between Oz and F8 and between O2 and Fp1, a trade-off reflecting the frontal areas more prominently activated to compensate for shortages in prosodic visual processing,[66] indicate additional

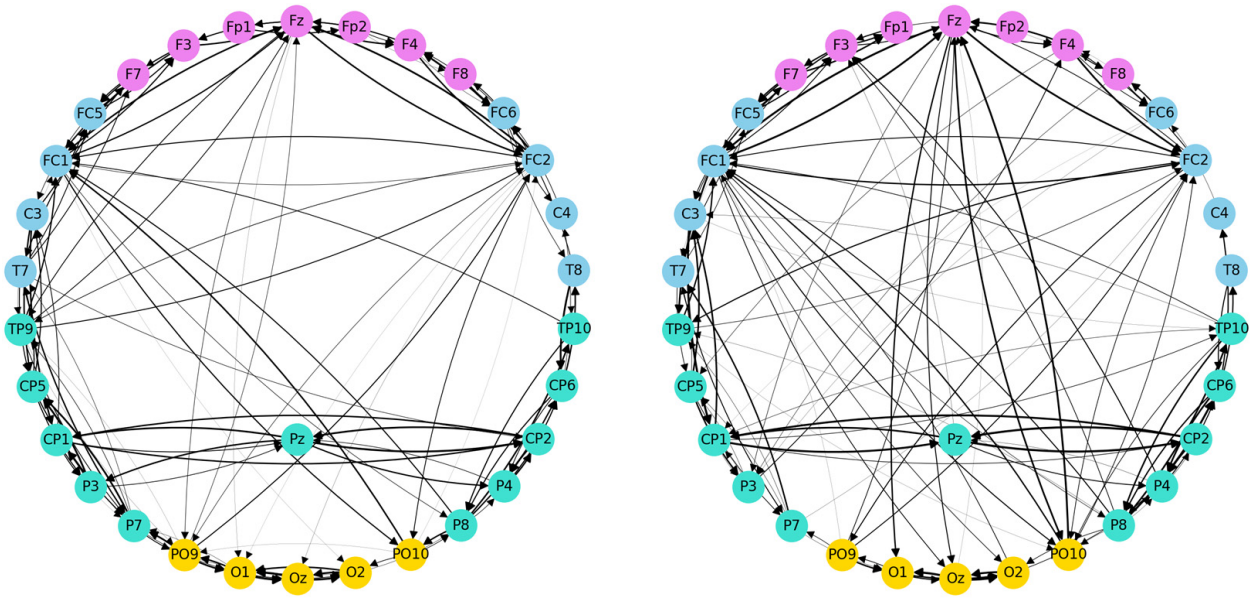

Fig. 3. Connectograms representing average causal activity for theta band for 4.8 Hz stimulus (left, control group, right, dyslexic group).

Table 2. GB classifier. Stimulus 4.8 Hz.

Band	Accuracy	AUC	Precision	Recall	*F*1-score
Delta	0.855	0.857	0.843	0.868	0.855
Theta	**0.896**	**0.929**	**0.893**	**0.899**	**0.896**
Alpha	0.865	0.891	0.858	0.872	0.865
Beta	0.865	0.879	0.857	0.873	0.865
Gamma	**0.865**	**0.911**	**0.864**	**0.866**	**0.865**

Table 3. GB classifier. Stimulus 4.8 Hz. Hyperparameters.

Band	Features set size	ntrees	max_depth	min_rows	learn_rate	sample_rate	c_sam._rate
Delta	40	100	3	10	0.05	0.6	0.6
Theta	**40**	**200**	**7**	**5**	**0.01**	**0.8**	**0.8**
Alpha	35	100	5	5	0.01	0.8	0.6
Beta	45	200	3	5	0.05	0.8	0.8
Gamma	**40**	**500**	**5**	**1**	**0.001**	**0.9**	**0.8**

cognitive effort to integrate speech rhythm and intonation. As shown in Fig. 5, these interactions stand out in the feature scores ranking, highlighting their potential compensatory role. This cognitive restructuring, which tries to compensate for dysfunction in visual areas, leads to increased cognitive load, affecting the recognition of prosodic speech impulses.[25,67] On the other hand, changes in the connection between C4 and F7, along with the interaction between Fp1 and C3, highlight problems in sensory and auditory synchronization, as well as in motor planning.

Figure 6 offers a connectogram-based visualization of these most influential causal links. These problems of theta synchronization could indicate a lack of coordination between attention and motor processes, which could explain the problems of speech and precision.[26,68]

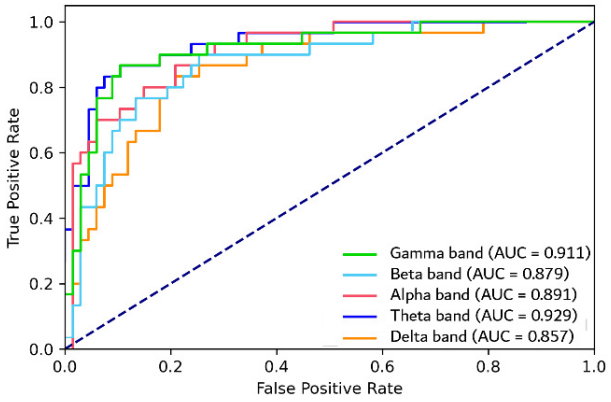

Fig. 4. ROC curves of GB classifier under 4.8 Hz stimulus.

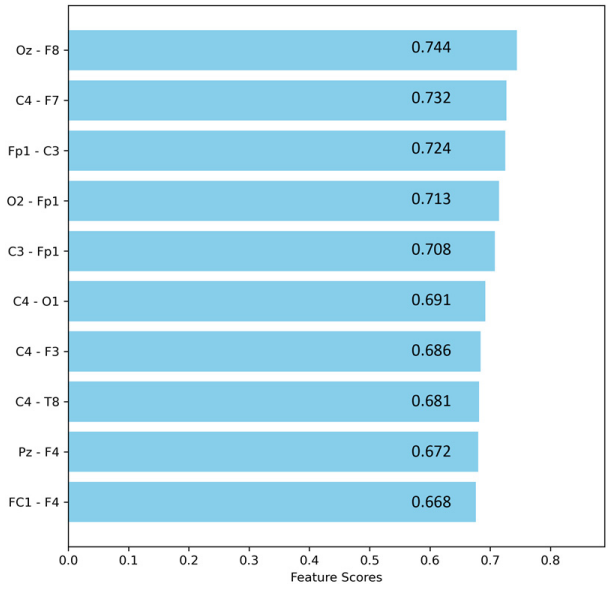

Fig. 5. Feature scores ranking. Theta band, 4.8 Hz.

The analysis of the gamma band shows crucial differences in functional connectivity between persons with dyslexia and controls, highlighting the importance of this band in prosodic language processing. The gamma band facilitates rapid neural synchronization between different brain areas, essential to the sensory and cognitive integration required to decode prosody, including pitch, rhythm, and intonation variations. The changes in gamma coherence observed in people with dyslexia suggest an impairment in the brain's ability to efficiently integrate and process prosodic information, which might explain their difficulties in understanding and producing prosodic language.[28,67]

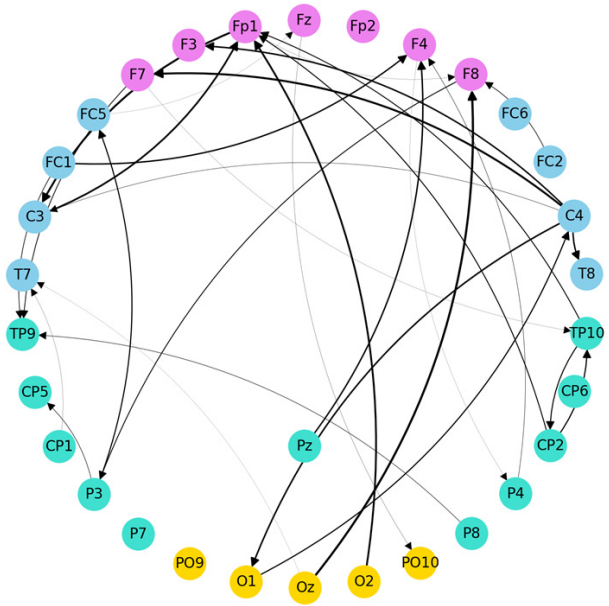

Fig. 6. Feature scores in connectogram. Theta band, 4.8 Hz.

As illustrated in Fig. 7, these connectivity changes appear prominently in changes in the connections between O2 and P4, and O1 and T7, in particular, indicate dysfunction in visual and prosodic integration. This suggests that problems in gamma synchronization can affect the ability of dyslexic individuals to coordinate visual and auditory signals

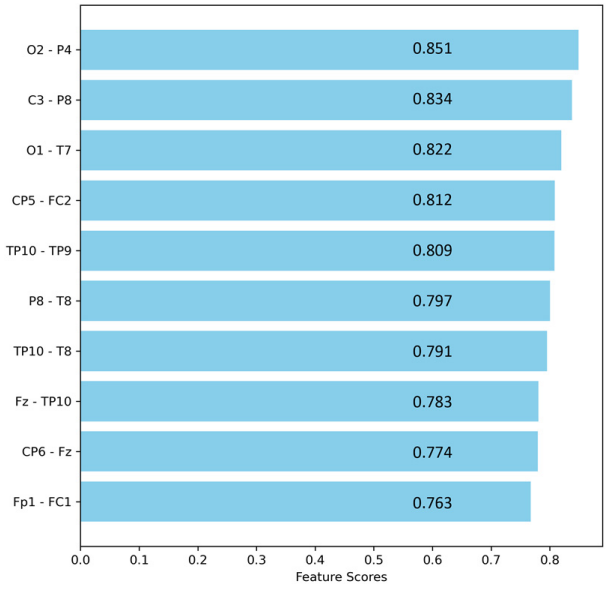

Fig. 7. Feature scores ranking. Gamma band, 4.8 Hz.

during prosody perception, a negative influence on fluidity and accuracy in prosodic understanding.[15,29,69] The lack of coordination between C3 and P8 and between Cp5 and FC2 highlights the problems of sensory and auditory integration in dyslexics. Figure 8 provides a connectogram-based visualization of these interactions, demonstrating how these changes reflect difficulties in synchronizing sensory and motor processes necessary for the correct interpretation and articulation of rhythm and intonation, dysfunction in these areas suggests that the gamma band does not sufficiently integrate multisensory information, contributing to the characteristic difficulties in understanding and producing prosodic language in dyslexia.[70]

4.2. *Stimulus at 40 Hz (Phoneme)*

Classification with causalities of EEG signals collected under a 40 Hz stimulus yields a similar result. The bands in which the highest performance is observed are equally theta and gamma, as can be seen in Table 4, and graphically, the ROC curves in Fig. 9. The appropriate choice of hyperparameters refines the performance obtained, illustrated in Table 5.

During the observation of a 40 Hz stimulus, the theta band is essential for time encoding and

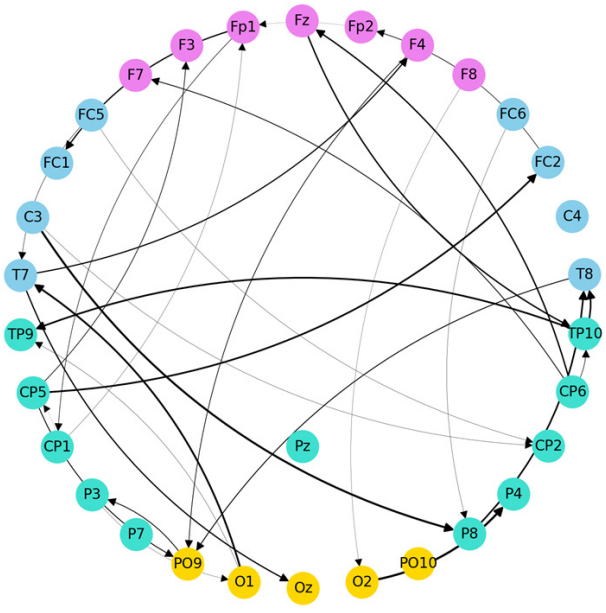

Fig. 8. Feature scores in connectogram. Gamma band, 4.8 Hz.

Table 4. GB classifier. Stimulus 40 Hz.

Band	Accuracy	AUC	Precision	Recall	*F*1-score
Delta	0.804	0.837	0.782	0.828	0.804
Theta	**0.824**	**0.849**	**0.816**	**0.831**	**0.824**
Alpha	0.814	0.822	0.795	0.835	0.814
Beta	0.793	0.813	0.779	0.809	0.793
Gamma	**0.855**	**0.892**	**0.848**	**0.864**	**0.855**

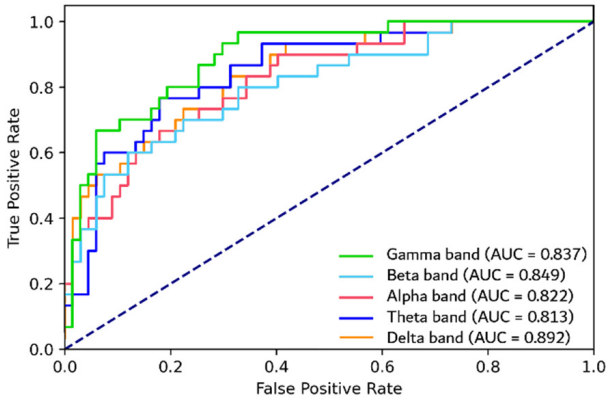

Fig. 9. ROC curves of GB classifier under 40 Hz stimulus.

interhemispheric synchronization, allowing the brain to maintain a continuous and coherent flow of phonological processing. In persons with dyslexia, theta band dysfunction can affect the accuracy of decoding and leading to language impairment.[20,22]

The changes in theta synchronization observed between the T8 and Fp1 electrodes and between Fp1 and C4 reveal a critical dysfunction in the ability of the dyslexic brain to integrate auditory phoneme signals with the executive and motor responses needed for their processing.[71] As shown in Fig. 10, these anomalies in theta-band connectivity stand out prominently in the feature ranking; these compounds suggest that the theta band, (responsible for this temporal synchronization), is affected, manifesting in a lack of coordination between phonological observation and motor planning. This may explain problems in expressing speech and persistent attention to phonological signals, affecting verbal fluency in persons with dyslexia.[72,73] In addition, the desynchronization between F3 and F8, along with the change in theta relationship between Cp5 and Pz, suggests a dysfunction in interhemispheric coordination and multisensory integration, which affects

Table 5. GB classifier. Stimulus 40 Hz. Hyperparameters.

Band	Features set size	ntrees	max_depth	min_rows	learn_rate	sample_rate	c_sam._rate
Delta	30	100	5	10	0.05	0.8	0.6
Theta	**45**	**200**	**7**	**5**	**0.01**	**0.8**	**0.8**
Alpha	40	100	3	5	0.05	0.9	0.6
Beta	45	50	7	10	0.10	0.6	0.8
Gamma	**45**	**500**	**5**	**1**	**0.001**	**0.9**	**0.8**

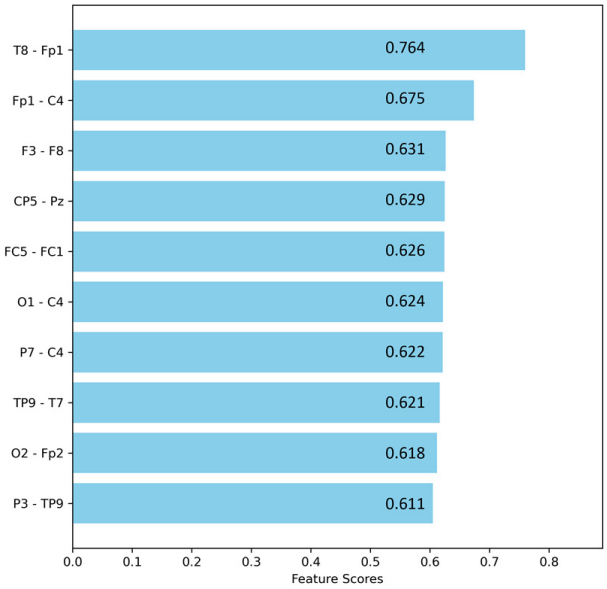

Fig. 10. Feature scores ranking. Theta band, 40 Hz.

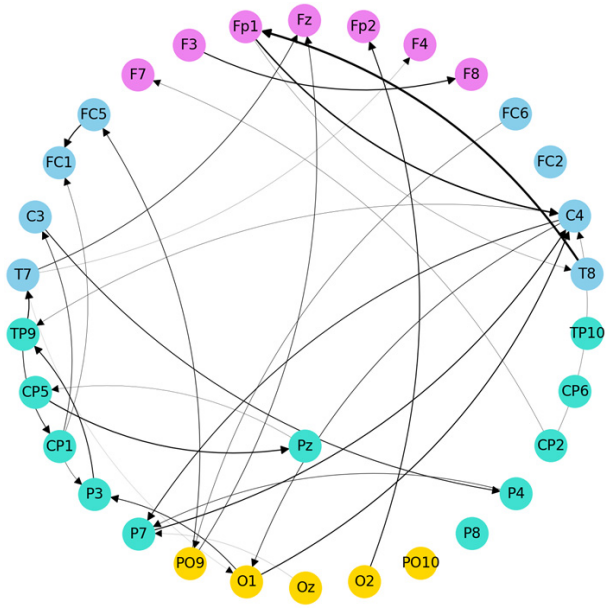

Fig. 11. Feature scores in connectogram. Theta band, 40 Hz.

the ability to process fast sequences of phonemes. Figure 11 provides a connectogram-based visualization of these compromised pathways, highlighting how these changes in theta synchronization not only disrupt the continuous perception of speech flow but also reflect a broader deficiency in the integration of sensory and cognitive information, crucial to the correct interpretation and production of language in individuals with dyslexia.[65,74]

Analysis of brain activity in response to a 40 Hz stimulus associated with phoneme perception shows significant differences in functional connectivity in the gamma band between individuals with dyslexia and the control group. This band is essential for the rapid synchronization of neuronal activity, enabling the efficient integration of sensory and cognitive information necessary for accurate and clear observation of phonemes. This timing is crucial for effective sound processing.[28]

In people with dyslexia, substantial changes in gamma synchronization between compounds O2–T8 and T8–O2 are stated, indicating a dysfunction in the integration of visual and auditory signals in perception. As illustrated in Fig. 12, these alterations are evident in the feature ranking, revealing a decrease in gamma coherence may indicate difficulties in coordination between visual perception and auditory signals, affecting the proper phonological decoding.[75] In addition, the relationship between PO10 and F8 is also relevant, reflecting problems in integrating visual information with executive functions necessary for real-time attention and phonetic discrimination. This lack of coordination may affect the ability of people with dyslexia to follow phonological signals, affecting language fluency.[76] The change in gamma synchronization in the relationship

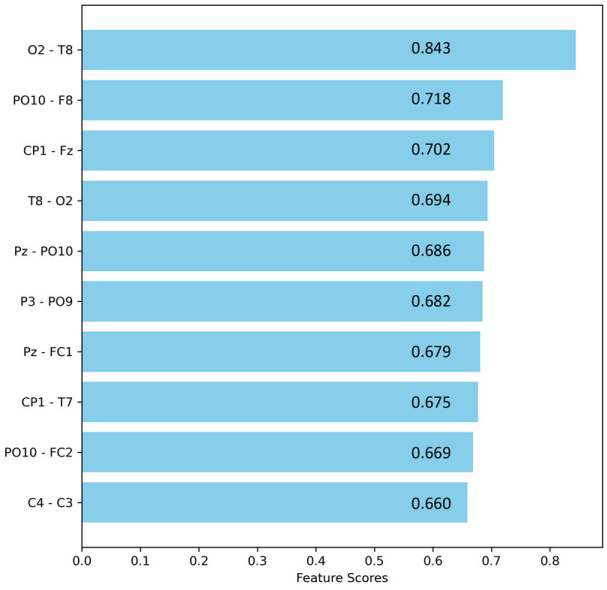

Fig. 12. Feature scores ranking. Gamma band, 40 Hz.

between Cp1 and Fz indicates problems in sensory and motor integration, fundamental to the precise articulation of phonemes. Figure 13 presents a connectogram visualization of these altered interactions, highlighting how the gamma band contributes to fluid speech production by not achieving sufficient synchronization between these areas, thus exacerbating the phonal difficulties of dyslexia.[77]

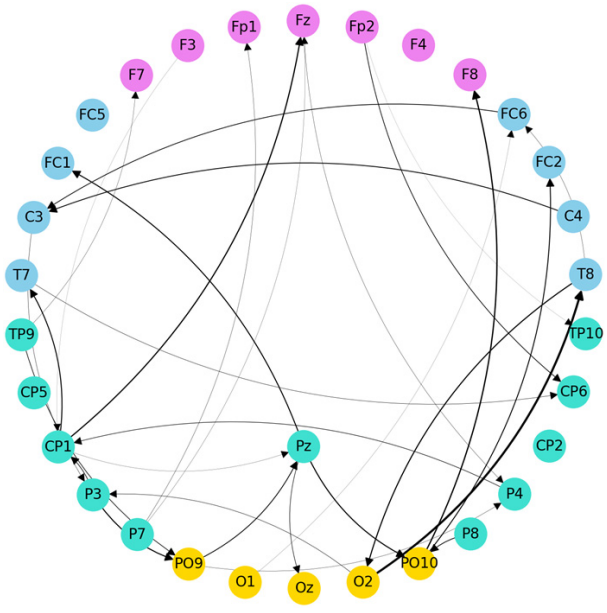

Fig. 13. Feature scores in connectogram. Gamma band, 40 Hz.

4.3. *Interpretation according to the TSF*

The findings in the functional connectivity of the theta and gamma bands in response to different stimuli reinforce Goswami's TSF theory,[15] which posits that difficulties in dyslexia arise from atypical neural oscillations in different frequency bands, affecting the temporal processing of auditory and phonological information. The interaction between the theta and gamma bands is especially relevant in this context, as slower theta oscillations can influence the timing of faster gamma oscillations. This atypical entrainment between both bands could explain how alterations in theta can generate cascading effects in gamma, affecting prosodic processing at multiple levels, from syllabic to phonological structure.[22] Taken together, these findings extend the applicability of TSF to the domain of theta and gamma oscillations in prosodic processing, suggesting that difficulties in dyslexia involve not only integration at low frequencies but also at higher frequencies. This results in a deficient integration of auditory, sensory, and motor information necessary for the perception and production of prosody, constituting an important neural marker for understanding the mechanisms underlying prosodic difficulties in dyslexia.

4.4. *Interpretation according to PCDH*

Alterations in the theta band under 4.8 Hz stimulation (focusing on prosody) suggest that individuals with dyslexia experience difficulties segmenting and orchestrating speech rhythm from the early stages of linguistic perception.[64] The phonological hypothesis[16] posits that the absence of a clear representation of speech sounds destabilizes temporal synchronization for detecting syllabic contours and intonation, thus requiring greater frontal activity (e.g. Oz–F8 or C4–F7) to compensate for the integrative role typically performed by occipitotemporal areas.[63] In parallel, gamma-band anomalies (also at 4.8 Hz) reinforce the notion of a fragile phonological framework: this band is crucial for rapid consolidation of auditory and visual cues, and its dysregulation (e.g. O2–P4, C3–P8, Cp5–FC2) indicates that the dyslexic individual struggles to effectively link prosodic signals with visual information, thus hindering speech planning and fluency.[78]

Data obtained at 40 Hz, commonly linked to phonemic processing, reveal similar patterns. A less

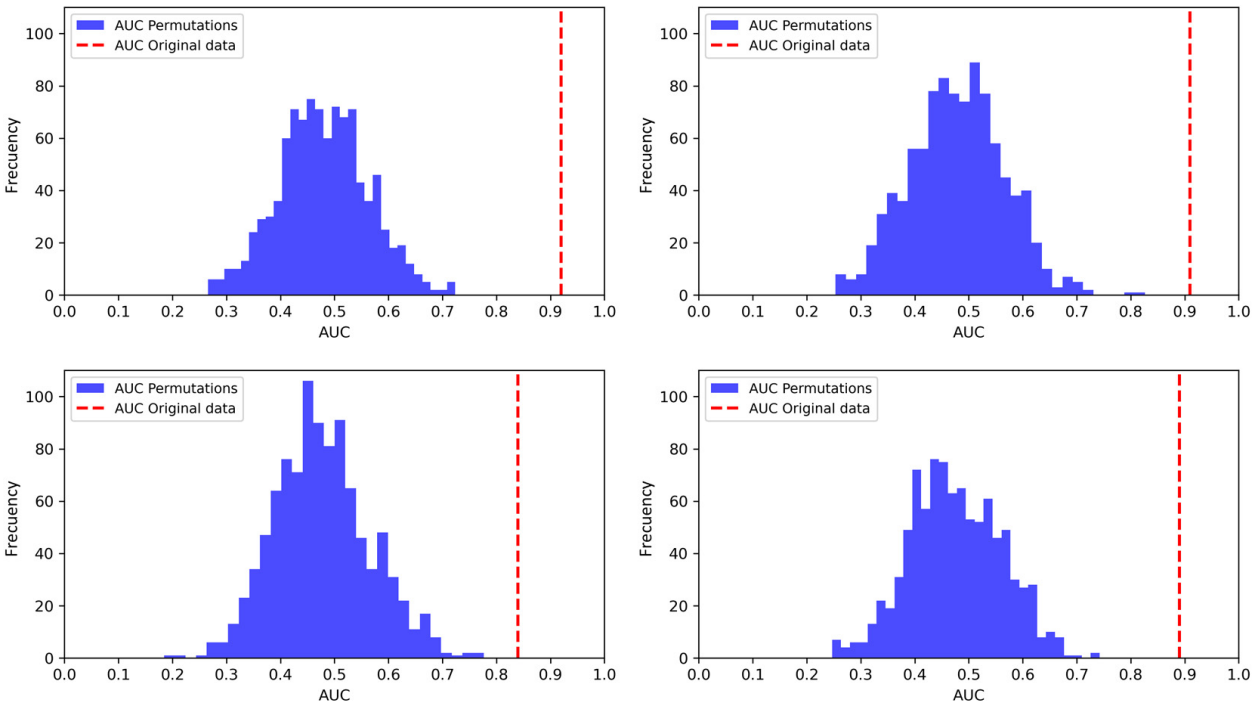

Fig. 14. Permutation tests. Left column, theta band. Right column, gamma band. First row, 4.8 Hz stimulus. Second row, 40 Hz stimulus.

robust gamma synchronization (e.g. T8–O2 or PO10–F8) reflects difficulties integrating and discriminating phonemes in real time, pointing to an unstable phonological encoding.[71] Furthermore, under these same 40 Hz conditions, the theta band shows anomalies in phoneme sequencing and motor verification (T8–Fp1 or F3–F8), again aligning with the phonological hypothesis, which proposes a deficit in the temporal alignment of sounds.[25]

By integrating both types of stimuli (4.8 Hz and 40 Hz) and examining their effects in theta and gamma bands, we see a convergent picture: phonological weakness transcends mere phoneme recognition, compromising temporal coherence and rapid audio-visual integration, revealing that the dyslexic brain strives to shore up a "fragile phonological core", affecting both prosodic and phonemic processing.[16]

It has been taken into account that the sample is relatively small and unbalanced, as is usual in real biomedical research. Additional statistical checks are desirable to ensure that the results are robust. Therefore, the classification has been performed under a permutation test of 1000 label variations, resulting in a distribution that assumes the null hypothesis, against the actual classification. Figure 14 shows the results of these tests with respect to the AUC, the true performance being marked with a red line. In all cases studied (4.8 Hz and 40 Hz stimuli, theta and gamma bands), the p-values are < 0.001.

5. Conclusion and Future Works

This study presents a novel approach to understanding the neural mechanisms underlying DD by analyzing EEG functional connectivity patterns elicited by specific auditory stimuli. By employing white noise modulated at 4.8 Hz and 40 Hz — frequencies corresponding to prosodic and phonemic elements of speech — we could isolate and examine the brain's oscillatory responses in individuals with dyslexia compared to controls. The application of the Hilbert transform allowed for the extraction of instantaneous phase information from EEG signals, which was crucial for constructing GC matrices representing directed and weighted interactions between brain regions.

Using the MICC for FS, we effectively identified the most informative EEG causal relationships and minimized redundancy. By combining MI and PCC, MICC has enabled us to focus on relations that were

both very relevant to the classification task and less related to each other. The GB classifier showed high accuracy and AUC values, especially in theta and gamma bands, through optimized hyperparameters and cross-validation. This indicates that oscillating activity in these frequency bands is particularly discriminatory for the distinction between dyslexic and expert readers.

Visualizing EEG connectivity via connectograms gave insightful representations of the complex neural networks involved. In particular, we have observed significant differences in functional connectivity patterns within the theta and gamma bands between the dyslexic and controls. These differences were consistent with TSF proposed by Goswami, which states that dyslexia arises from atypical neural oscillations that disrupt the temporal processing of auditory and phonological information. In particular, our findings suggest that abnormalities in theta–gamma coupling can contribute to the phonological and prosodic difficulties experienced by individuals with dyslexia.

By integrating advanced signal processing techniques, robust FS, machine learning classification and advanced visualization methods, this research provides a comprehensive framework for analyzing EEG data in the context of dyslexia. The identification of specific neural connectivity patterns associated with DD not only improves our understanding of the neurophysiologist basis, but also provides potential biomarkers for early diagnosis. Future work should aim to validate these findings in larger and more diverse populations to take into account variability between different age groups and linguistic backgrounds. Longitudinal studies could investigate how these neural connectivity patterns evolve with intervention or over development time scales. In addition, examining the applicability of this methodology to other neurological or learning disorders may provide a broader understanding of the generalization of these techniques.

Acknowledgments

This research is part of the PID2022-137461NBC32, PID2022-137629OA-I00, and PID2022-137451OB-I00 projects, funded by MICIU/AEI/10.13039/501100011033 and by ERDF/EU, and the University of Málaga (UMA), BioSiP (TIC-251), and Leeduca research groups. Work by I.R.-R. is part of the grant RYC2023-045296-I funded by MICIU/AEI/10.13039/501100011033 and by ESF+.

ORCID

Ignacio Rodríguez-Rodríguez https://orcid.org/0000-0002-0118-3406
José Ignacio Mateo-Trujillo https://orcid.org/0009-0005-2156-3587
Andrés Ortiz https://orcid.org/0000-0003-2690-1926
Nicolás J. Gallego-Molina https://orcid.org/0000-0002-6536-9234
Diego Castillo-Barnes https://orcid.org/0000-0003-1635-5685
Juan L. Luque https://orcid.org/0000-0003-2559-3896

References

1. R. L. Peterson and B. F. Pennington, Developmental dyslexia, *Lancet* **379** (2012) 1997–2007.
2. P. A. Thompson, C. Hulme, H. M. Nash, D. Gooch, E. Hayiou-Thomas and M. J. Snowling, Developmental dyslexia: Predicting individual risk, *J. Child Psychol. Psychiatry* **56** (2015) 976–987.
3. L. Zuppardo, F. Serrano, C. Pirrone and A. Rodriguez-Fuentes, More than words: Anxiety, self-esteem, and behavioral problems in children and adolescents with dyslexia, *Learn. Disabil. Q.* **46** (2023) 77–91.
4. N. J. Gallego-Molina, A. Ortiz, F. J. Martínez-Murcia, I. Rodríguez-Rodríguez and J. L. Luque, Assessing functional brain network dynamics in dyslexia from FNIRS data, *Int. J. Neural Syst.* **33** (2023) 2350017.
5. K. A. Clark *et al.*, Neuroanatomical precursors of dyslexia identified from pre-reading through to age 11, *Brain* **137** (2014) 3136–3141.
6. E. Cainelli, L. Vedovelli, B. Carretti and P. Bisiacchi, EEG correlates of developmental dyslexia: A systematic review, *Ann. Dyslexia* **73** (2023) 184–213.
7. M. Chaturvedi *et al.*, Phase lag index and spectral power as QEEG features for identification of patients with mild cognitive impairment in Parkinson's disease, *Clin. Neurophysiol.* **130** (2019) 1937–1944.
8. M. Ahmadlou, A. Adeli, R. Bajo and H. Adeli, Complexity of functional connectivity networks in mild cognitive impairment subjects during a working memory task, *Clin. Neurophysiol.* **125** (2014) 694–702.
9. M. A. Yaqub, K. S. Hong, A. Zafar and C. S. Kim, Control of transcranial direct current stimulation duration by assessing functional connectivity of near-infrared spectroscopy signals, *Int. J. Neural Syst.* **32** (2022) 2150050.

10. F. J. Martinez-Murcia *et al.*, EEG connectivity analysis using denoising autoencoders for the detection of dyslexia, *Int. J. Neural Syst.* **30** (2020) 2050037.
11. H. Osterhage, F. Mormann, T. Wagner and K. Lehnertz, Measuring the directionality of coupling: Phase versus state space dynamics and application to EEG time series, *Int. J. Neural Syst.* **17** (2007) 139–148.
12. M. Ding, Y. Chen and S. L. Bressler, Granger causality: Basic theory and application to neuroscience, in *Handbook of Time Series Analysis: Recent Theoretical Developments and Applications* (Wiley, 2006), pp. 437–460.
13. G. Žarić *et al.*, Altered patterns of directed connectivity within the reading network of dyslexic children and their relation to reading dysfluency, *Dev. Cogn. Neurosci.* **23** (2017) 1–13.
14. N. Kwak and C. H. Choi, Input feature selection for classification problems, *IEEE Trans. Neural Netw.* **13** (2002) 143–159.
15. U. Goswami, A temporal sampling framework for developmental dyslexia, *Trends Cogn. Sci.* **15** (2011) 3–10.
16. A. Castles and N. Friedmann, Developmental dyslexia and the phonological deficit hypothesis, *Mind Lang.* **29** (2014) 270–285.
17. A. De Vos, S. Vanvooren, J. Vanderauwera, P. Ghesquière and J. Wouters, Atypical neural synchronization to speech envelope modulations in dyslexia, *Brain Lang.* **164** (2017) 106–117.
18. D. Coluzzi *et al.*, Development and testing of spidernet: An interactive tool for brain connectogram visualization, sub-network exploration and graph metrics quantification, *Front. Neurosci.* **16** (2022) 818385.
19. E. Bullmore and O. Sporns, Complex brain networks: Graph theoretical analysis of structural and functional systems, *Nat. Rev. Neurosci.* **10** (2009) 186–198.
20. A. J. Power, L. J. Colling, N. Mead, L. Barnes and U. Goswami, Neural encoding of the speech envelope by children with developmental dyslexia, *Brain Lang.* **160** (2016) 1–10.
21. U. Goswami, N. Mead, T. Fosker, M. Huss, L. Barnes and V. Leong, Impaired perception of syllable stress in children with dyslexia: A longitudinal study, *J. Mem. Lang.* **69** (2013) 1–17.
22. V. Leong and U. Goswami, Assessment of rhythmic entrainment at multiple timescales in dyslexia: Evidence for disruption to syllable timing, *Hear. Res.* **308** (2014) 141–162.
23. G. Rippon and N. Brunswick, Trait and state EEG indices of information processing in developmental dyslexia, *Int. J. Psychophysiol.* **36** (2000) 251–265.
24. G. M. Di Liberto, V. Peter, M. Kalashnikova, U. Goswami, D. Burnham and E. C. Lalor, Atypical cortical entrainment to speech in the right hemisphere underpins phonemic deficits in dyslexia, *NeuroImage* **175** (2018) 70–79.
25. G. Mai, J. W. Minett and W. S. Y. Wang, Delta, theta, beta, and gamma brain oscillations index levels of auditory sentence processing, *NeuroImage* **133** (2016) 516–528.
26. S. M. Doesburg, S. A. Vinette, M. J. Cheung and E. W. Pang, Theta-modulated gamma-band synchronization among activated regions during a verb generation task, *Front. Psychol.* **3** (2012) 195.
27. L. Wang, Z. Zhu and M. Bastiaansen, Integration or predictability? Further specification of the functional role of EEG gamma-band oscillations during language comprehension, *Front. Psychol.* **3** (2012) 00187.
28. P. Fries, Rhythms for cognition: Communication through coherence, *Neuron* **88** (2015) 220–235.
29. L. H. Arnal and A. L. Giraud, Cortical oscillations and sensory predictions, *Trends Cogn. Sci.* **16** (2012) 390–398.
30. V. Sakkalis, Review of advanced techniques for the estimation of brain connectivity measured with EEG/MEG, *Comput. Biol. Med.* **41** (2011) 1110–1117.
31. I. Rodríguez-Rodríguez, A. Ortiz, N. J. Gallego-Molina, M. A. Formoso and W. L. Woo, EEG interchannel causality to identify source/sink phase connectivity patterns in developmental dyslexia, *Int. J. Neural Syst.* **33** (2023) 2350020.
32. S. A. Unde and R. Shriram, Coherence analysis of EEG signal using power spectral density, in *2014 Fourth Int. Conf. Communication Systems and Network Technologies* (IEEE, 2014), pp. 871–874.
33. F. Mormann, K. Lehnertz, P. David and C. E. Elger, Mean phase coherence as a measure for phase synchronization and its application to the EEG of epilepsy patients, *Physica D* **144** (2000) 358–369.
34. Y. Gao, X. Wang, T. Potter, J. Zhang and Y. Zhang, Single-trial EEG emotion recognition using Granger causality/transfer entropy analysis, *J. Neurosci. Methods* **346** (2020) 108904.
35. T. Uchida, K. Fujiwara, T. Inoue, Y. Maruta, M. Kano and M. Suzuki, Analysis of VNS effect on EEG connectivity with Granger causality and graph theory, in *2018 Asia-Pacific Signal and Information Processing Association Annual Summit and Conf. (APSIPA ASC)* (IEEE, 2018), pp. 861–864.
36. D. Marinazzo, W. Liao, H. Chen and S. Stramaglia, Nonlinear connectivity by Granger causality, *NeuroImage* **58** (2011) 330–338.
37. R. Guha, K. K. Ghosh, S. Bhowmik and R. Sarkar, Mutually informed correlation coefficient (MICC)-A new filter based feature selection method, in *2020 IEEE Calcutta Conf. (CALCON)* (IEEE, 2020), pp. 54–58.
38. G. F. González *et al.*, Graph analysis of EEG resting state functional networks in dyslexic readers, *Clin. Neurophysiol.* **127** (2016) 3165–3175.
39. J. Bosch-Bayard, K. Girini, R. J. Biscay, P. Valdes-Sosa, A. C. Evans and G. A. Chiarenza, Resting EEG effective connectivity at the sources in developmental

dysphonetic dyslexia: Differences with non-specific reading delay, *Int. J. Psychophysiol.* **153** (2020) 135–147.
40. Z. Sankari, H. Adeli and A. Adeli, Wavelet coherence model for diagnosis of Alzheimer disease, *Clin. EEG Neurosci.* **43** (2012) 268–278.
41. H. C. Baggio *et al.*, Functional brain networks and cognitive deficits in Parkinson's disease, *Hum. Brain Mapp.* **35** (2014) 4620–4634.
42. R. Yuvaraj, M. Murugappan, U. R. Acharya, H. Adeli, N. M. Ibrahim and E. Mesquita, Brain functional connectivity patterns for emotional state classification in Parkinson's disease patients without dementia, *Behav. Brain Res.* **298** (2016) 248–260.
43. G. J. Ji, Y. Yu, H. H. Miao, Z. J. Wang, Y. L. Tang and W. Liao, Decreased network efficiency in benign epilepsy with centrotemporal spikes, *Radiology* **283** (2017) 186–194.
44. M. Ahmadlou and H. Adeli, Complexity of weighted graph: A new technique to investigate structural complexity of brain activities with applications to aging and autism, *Neurosci. Lett.* **650** (2017) 103–108.
45. V. Blasi *et al.*, Early life adversities and borderline intellectual functioning negatively impact limbic system connectivity in childhood: A connectomics-based study, *Front. Psychiatry* **11** (2020) 497116.
46. M. Ahmadlou, H. Adeli and A. Adeli, Spatiotemporal analysis of relative convergence of EEGs reveals differences between brain dynamics of depressive women and men, *Clin. EEG Neurosci.* **44** (2013) 175–181.
47. A. Ortiz, F. J. Martinez-Murcia, J. L. Luque, A. Giménez, R. Morales-Ortega and J. Ortega, Dyslexia diagnosis by EEG temporal and spectral descriptors: An anomaly detection approach, *Int. J. Neural Syst.* **30** (2020) 2050029.
48. R. Pauc, Comorbidity of dyslexia, dyspraxia, attention deficit disorder (ADD), attention deficit hyperactive disorder (ADHD), obsessive compulsive disorder (OCD) and Tourette's syndrome in children: A prospective epidemiological study, *Clin. Chiropr.* **8** (2005) 189–198.
49. M. Lizarazu *et al.*, Developmental evaluation of atypical auditory sampling in dyslexia: Functional and structural evidence, *Hum. Brain Mapp.* **36** (2015) 4986–5002.
50. K. Lehongre, F. Ramus, N. Villiermet, D. Schwartz and A. L. Giraud, Altered low-gamma sampling in auditory cortex accounts for the three main facets of dyslexia, *Neuron* **72** (2011) 1080–1090.
51. J. A. Hämäläinen, H. K. Salminen and P. H. T. Leppänen, Basic auditory processing deficits in dyslexia: Systematic review of the behavioral and event-related potential/field evidence, *J. Learn. Disabil.* **46** (2013) 413–427.
52. R. Li and J. C. Principe, Blinking artifact removal in cognitive EEG data using ICA, in *2006 Int. Conf. IEEE Engineering in Medicine and Biology Society* (IEEE, 2006), pp. 5273–5276.
53. D. G. E. Robertson and J. J. Dowling, Design and responses of Butterworth and critically damped digital filters, *J. Electromyogr. Kinesiol.* **13** (2003) 569–573.
54. C. W. J. Granger, Investigating causal relations by econometric models and cross-spectral methods, *Econometrica* **37** (1969) 424–438.
55. H. Akaike, A new look at the statistical model identification, *IEEE Trans. Autom. Control* **19** (1974) 716–723.
56. E. Atukeren, The relationship between the F-test and the Schwarz criterion: Implications for Granger-causality tests, *Econ. Bull.* **30** (2010) 494–499.
57. F. Hu, H. Wang, Q. Wang, N. Feng, J. Chen and T. Zhang, Acrophobia quantified by EEG based on CNN incorporating Granger causality, *Int. J. Neural Syst.* **31** (2021) 2050069.
58. X. Wang, Y. Chen, S. L. Bressler and M. Ding, Granger causality between multiple interdependent neurobiological time series: Blockwise versus pairwise methods, *Int. J. Neural Syst.* **17** (2007) 71–78.
59. B. Seijo-Pardo, I. Porto-Díaz, V. Bolón-Canedo and A. Alonso-Betanzos, Ensemble feature selection: Homogeneous and heterogeneous approaches, *Knowl.-Based Syst.* **118** (2017) 124–139.
60. J. H. Friedman, Stochastic gradient boosting, *Comput. Stat. Data Anal.* **38** (2002) 367–378.
61. D. F. Salisbury and G. Taylor, Semantic priming increases left hemisphere theta power and intertrial phase synchrony, *Psychophysiology* **49** (2012) 305–311.
62. D. Poeppel, The analysis of speech in different temporal integration windows: Cerebral lateralization as 'asymmetric sampling in time', *Speech Commun.* **41** (2003) 245–255.
63. D. Poeppel, The neuroanatomic and neurophysiological infrastructure for speech and language, *Curr. Opin. Neurobiol.* **28** (2014) 142–149.
64. D. Wildgruber, T. Ethofer, D. Grandjean and B. Kreifelts, A cerebral network model of speech prosody comprehension, *Int. J. Speech Lang. Pathol.* **11** (2009) 277–281.
65. C. Spironelli and A. Angrilli, Developmental aspects of language lateralization in delta, theta, alpha and beta EEG bands, *Biol. Psychol.* **85** (2010) 258–267.
66. N. Taran *et al.*, The role of visual attention in dyslexia: Behavioral and neurobiological evidence, *Hum. Brain Mapp.* **43** (2022) 1720–1737.
67. M. Keshavarzi, M. Kegler, S. Kadir and T. Reichenbach, Transcranial alternating current stimulation in the theta band but not in the delta band modulates the comprehension of naturalistic speech in noise, *NeuroImage* **210** (2020) 116557.

68. Y. Pu, D. Cheyne, Y. Sun and B. W. Johnson, Theta oscillations support the interface between language and memory, *NeuroImage* **215** (2020) 116782.
69. F. Artoni *et al.*, High gamma response tracks different syntactic structures in homophonous phrases, *Sci. Rep.* **10** (2020) 7537.
70. S. M. Doesburg, A. B. Roggeveen, K. Kitajo and L. M. Ward, Large-scale gamma-band phase synchronization and selective attention, *Cereb. Cortex* **18** (2008) 386–396.
71. A. Widmann, E. Schröger, M. Tervaniemi, S. Pakarinen and T. Kujala, Mapping symbols to sounds: Electrophysiological correlates of the impaired reading process in dyslexia, *Front. Psychol.* **3** (2012) 60.
72. A. L. Giraud and D. Poeppel, Cortical oscillations and speech processing: Emerging computational principles and operations, *Nat. Neurosci.* **15** (2012) 511–517.
73. W. Klimesch, EEG alpha and theta oscillations reflect cognitive and memory performance: A review and analysis, *Brain Res. Rev.* **29** (1999) 169–195.
74. E. S. Finn *et al.*, Disruption of functional networks in dyslexia: A whole-brain, data-driven analysis of connectivity, *Biol. Psychiatry* **76** (2014) 397–404.
75. A. L. Giraud and D. Poeppel, Speech perception from a neurophysiological perspective, in *The Human Auditory Cortex* (Springer, New York, 2012).
76. L. H. Arnal, V. Wyart and A. L. Giraud, Transitions in neural oscillations reflect prediction errors generated in audiovisual speech, *Nat. Neurosci.* **14** (2011) 797–801.
77. S. Cutini, D. Szücs, N. Mead, M. Huss and U. Goswami, Atypical right hemisphere response to slow temporal modulations in children with developmental dyslexia, *NeuroImage* **143** (2016) 40–49.
78. C. Spironelli, B. Penolazzi, C. Vio and A. Angrilli, Inverted EEG theta lateralization in dyslexic children during phonological processing, *Neuropsychologia* **44** (2006) 2814–2821.